

# Reconfigurable voltage source inverter for power factor correction of on-board chargers

Deepa Machadan Unni, Bindu Gopakumar Rajalekshmi

Department of Electrical Engineering, College of Engineering Trivandrum, APJ Abdul Kalam Technological University, Thiruvananthapuram, India

## Article Info

### Article history:

Received Jan 21, 2024

Revised May 29, 2024

Accepted Jun 2, 2024

### Keywords:

AC-DC rectifier

Bridgeless converter

Light electric vehicle

On-board charger

PFC converter

Voltage source inverter

## ABSTRACT

The effectiveness and efficiency of battery chargers are crucial for the performance of electric vehicles. The growing demand for electric vehicles warrants the development of chargers with better power factor, low distortion for the input current and low total harmonics distortion. An in-depth investigation of different configurations of power factor correction converters with the above features reveals the need for additional circuitry with existing chargers. Hence this paper focuses on reconfiguring the existing voltage source inverter of the propulsion motor drive of electric vehicles (EVs) to obtain a power factor correction converter by a novel switching scheme. A bridgeless boost topology is chosen based on the performance analysis of different power factor correction topologies done on a MATLAB-Simulink platform. The simulation results prove that the proposed reconfigurable front end converter improves the input current drawn by the electric vehicle charger and improves the power quality with a low value for total harmonic distortion of 6.56%. A switching scheme is then developed for the voltage source inverter to reconfigure it as a bridgeless boost power factor correction converter. This scheme result in a high value of 0.75 for the component utilisation factor thus proving its effectiveness as compared to existing schemes.

This is an open access article under the [CC BY-SA](#) license.



## Corresponding Author:

Deepa Machadan Unni

Department of Electrical Engineering, College of Engineering Trivandrum

APJ Abdul Kalam Technological University

Thiruvananthapuram, Kerala 695016, India

Email: deepashibu@cet.ac.in

## 1. INTRODUCTION

In recent years, the harmful effects of carbon emissions on the environment and human health have become more evident. This has led to finding alternative and more sustainable forms of transportation. The carbon emissions of internal combustion engines contribute to global warming, air pollution, and climate change. To address these issues, due to the zero emissions and lower operating costs, electric vehicles (EVs) are becoming increasingly popular [1]–[3]. As technology advances, the range of EVs is also improving and more electric vehicle models are being introduced with longer driving ranges, lower operating costs, and government incentives. These EVs are driven by a motor drive powered by the high power density battery placed inside the vehicle [4], [5]. In the case of India, a large portion of the vehicle population consists of two and three wheelers. The batteries of light electric vehicles (LEVs) such as two and three wheelers are charged from the domestic supply using an on-board charger (OBC) [6], [7].

EV chargers typically use a cascade combination of a front end AC-DC converter with a full bridge diode rectifier, which is followed by a DC-DC converter. These conventional chargers draw a highly distorted input current, thereby producing poor power quality issues, high total harmonics distortion (THD), and low efficiency. To improve the efficiency of the battery charging, a more realistic EV charger configuration with front end power factor correction (PFC) stage is essential [8]–[10]. Hence, front end PFC converter cascaded with an isolated DC-DC converter, which provides a constant voltage and constant current charging characteristics is required for battery charging. A diode bridge rectifier followed by a DC-DC non-isolated converter like a boost converter serves the purpose of power factor correction. In a diode bridge rectifier, the voltage stress acting on the diodes becomes significant due to the high switching frequency of the converter, producing increased power losses, and reduced converter efficiency [11]–[13]. Hence in recent years, bridgeless converters have gained attention as PFC converters due to their simple design, fewer switches, and high efficiency [14]–[16]. Various bridgeless configurations derived from basic DC-DC converter topologies such as boost and buck boost converters have been reported in previous research work. One of the additional advantages of these bridgeless configurations is that they eliminate the need for a front end diode bridge rectifier [17]–[20]. This paper mainly focuses on the power quality issues related to the process of EV charging. Moreover, an investigation of a switching scheme that can reconfigure the existing voltage source inverter of the traction motor drive as a battery charger will reduce the size of the charger as well as increase power density, which will be cost effective for LEVs [21]–[23].

From the literature survey, it is observed that in all previous investigations, a simple switching scheme that integrates battery charging operation into the traction drive is not done. Hence the design and analysis of a simple switching scheme to reconfigure the brushless direct current (BLDC) motor drive is to be derived to integrate propulsion and on-board battery charger operations. Considering the technological revolution occurring in the field of light electric vehicles, the design of a high power density, cost effective reconfigurable converter will be beneficial to future energy needs. A comprehensive study of different bridgeless topologies will reveal the features of each of these so that the best option can be adopted for front end PFC of OBC. Hence this paper focuses on the above comparison and a novel switching scheme for reconfiguration of three-phase voltage source inverter for battery charging is introduced.

This paper presents the basic block diagram of a two Stage OBC in section 2, this section provides an overview of the basic architecture of a two-stage OBC. The various bridgeless topologies and their principle of operation are discussed in section 3, it also includes the key components and design equations that need to be considered during the design process. The proposed switching scheme for the reconfiguration method is presented in section 4. The experimental verification is discussed in section 5. The performance comparison between different bridgeless topologies and detailed results and discussions are presented in section 6. The paper concludes by summarising the findings and discusses the implications of the research in the final, show in section 7.

## 2. STATE OF ART OF A TWO STAGE OBC-AN OVERVIEW

EV chargers are classified depending on the type of input power (DC, single phase AC, and three phase AC), range of power, speed of charging, charging time, and location of charger (on-board, off-board). Different types of EV charging level specifications in India are given in Table 1 [9], [24]. Level 1 and Level 2 AC chargers can operate from the single phase AC household power supply. LEVs use level 1 on-board charger (OBC) for battery charging. The type of battery charger decides the lifetime of the battery and its charging time [25]. The basic architecture of an OBC for LEV application is given in Figure 1.

Table 1. EV charging level specifications in India

Level	Supply	Voltage (V)	Max. power (kW)
Level 1	AC	240	3.5
	DC	48	15
Level 2	AC	380-400	22
Level 3	AC	200-1000	43
	DC	200-1000	400

The first stage is an AC-DC rectifier with a diode bridge rectifier followed by a Non-isolated DC-DC converter such as boost converter, buck boost converter, cuk converter, sepic converter, and zeta converter

which serves the function of power factor correction. An isolated DC-DC converter converts the high DC input voltage to the required level for charging the battery. The major design features of PFC converters are sinusoidal input current, better pf, low THD, high efficiency, high power density, less number of switches, and diodes. Unlike the conventional OBC for EVs detailed in this section, bridgeless configuration improves the efficiency of front end PFC converter. Hence a modified bridgeless topologies derived from conventional non-isolated PFC converters are discussed in the next section.

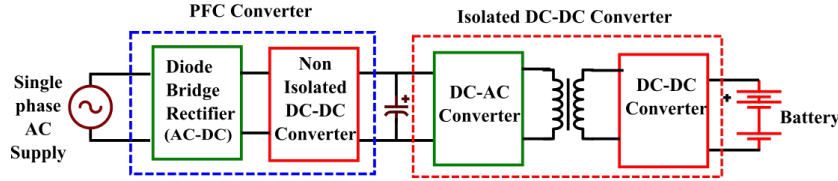


Figure 1. Basic architecture of two stage OBC for EVs

### 3. SINGLE PHASE NON-ISOLATED BRIDGELESS PFC CONVERTERS

Front end diode bridge rectifier and non-isolated DC-DC converter can be replaced with a bridgeless configuration of AC-DC rectifier, which improves the conversion efficiency. Bridgeless topology is derived from conventional boost or its derived converters. This section deals with the performance analysis of three PFC converters with bridgeless topology derived from boost and buck boost converters.

#### 3.1. Bridgeless buck boost converter

The bridgeless buck boost topology is derived from two single-switch buck boost converters operating in each half cycle of AC input supply as shown in Figure 2. Inductor  $L_1$  charges through  $Q_1$  and diode  $D_2$  and it discharges through  $D_3$  in positive half of the supply voltage when  $Q_1$  is off position. Similarly  $L_2$  charges through  $Q_2$  and diode  $D_1$  and it discharges through  $D_4$  in the negative half cycle. The value of inductance plays a crucial role in determining the mode of operation as either continuous conduction or discontinuous conduction [26]. Low power application uses discontinuous conduction because it requires less number of sensors. The design details of the front end bridgeless buck boost converter in discontinuous conduction mode with an output power of 500 W for an AC input voltage of 230 V and a DC output voltage of 400 V are included in Table 2.

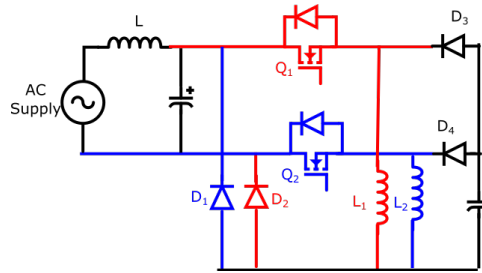


Figure 2. Bridgeless buck boost converter

Table 2. Design details of bridgeless buck boost converter

Parameters	Symbol	Design equation	Design values
Duty cycle	$d$	$d = \frac{V_{dc}}{V_{dc} + V_{in}}$	0.63
Critical input inductance	$L_{icmin}$	$L_{icmin} = \frac{V_{dcmin}^2 (1-d)^2}{P_{min} 2f_s}$	35 $\mu$ H
Output capacitor	$C_{dc}$	$C_{dc} = \frac{P_0 / V_{dcdes}}{2\omega \Delta V_{dc}}$	2200 $\mu$ F
Input filter capacitor	$C_{max}$	$C_{max} = \frac{I_{peak}}{\omega_L V_{peak}} \tan \theta$	330nF
Input filter inductor	$L_{req}$	$L_{req} = \frac{1}{4C_f \pi^2 f_{c,2} - L_s}$	1.57 mH

### 3.2. Bridgeless Luo converter

Voltage lifting and power factor correction features of Luo converter make it suitable to operate as an AC-DC rectifier [27]. The circuit diagram of the bridgeless Luo converter is given in Figure 3. By using two different switches for positive and negative half cycles, it is possible to control the flow of current and rectify the AC voltage to DC voltage using a bridgeless configuration. Switch  $Q_1$ , Diodes  $D_1$ , and  $D_3$  and inductor  $L_1$  and  $L_3$  are operating in positive cycle. Switch  $Q_2$ , Diodes  $D_2$ , and  $D_4$  and inductor  $L_2$  and  $L_4$  are operating in negative cycle.

In the positive cycle,  $L_1$  charges through switch  $Q_1$  and  $D_2$  and at that time the stored energy in the intermediate capacitor  $C_1$  is transferred to  $L_3$  and  $C_{dc}$ . The current in the output inductor and the DC link voltage are increased and the voltage across the intermediate capacitor  $C_1$  decreases. The input side inductor  $L_1$  transfers its energy to  $C_1$  through the diode  $D_3$  when switch  $Q_1$  is in off position. The voltage across the intermediate capacitor increases until the current  $i_{L1}$  decreases to zero. The DC link capacitor  $C_{dc}$  supplies energy to the second stage of OBC. Similarly  $Q_2$ ,  $L_2$ ,  $L_4$ , diode  $D_4$  and intermediate capacitor  $C_2$  are operating for the negative half cycle to attain the required output. Design values of bridgeless Luo converter are given in Table 3 [28],[29].

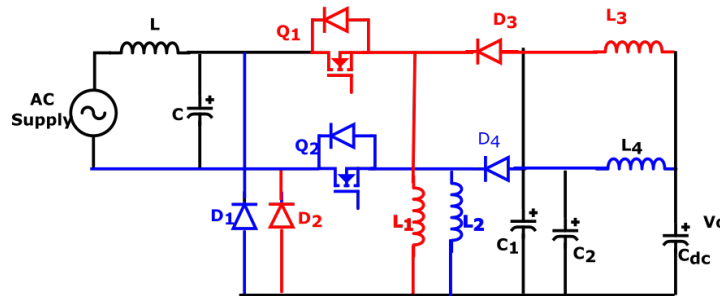


Figure 3. Bridgeless Luo converter

Table 3. Design parameters of bridgeless LUO converter

Parameters	Symbols	Design equations	Design values
Duty cycle	$d$	$d = \frac{V_{dc}}{V_{dc} + V_{in}}$	0.63
Critical input inductance	$L_{ic}$	$L_{ic} = \frac{d_{min}(1 + d_{min})V_{in}}{2I_0 f_s}$	40 $\mu$ H
Intermediate capacitance	$C_{12}$	$C_{in} = C_1 = C_2 = \frac{d_{max} V_c}{2f_s R_L (\Delta V_c)/2}$	0.44 $\mu$ F
Intermediate inductance	$L_{012}$	$L_{0,1,2} = \frac{d_{max} I_0}{16f_s^2 C_{in} (\Delta I_0)/2}$	1.78 mH
Output capacitor	$C_{dc}$	$C_{dc} = \frac{I_0}{2\omega_L (\Delta V_{dcmin})}$	2200 $\mu$ F

### 3.3. Bridgeless boost converter

The front end AC-DC rectifier using bridgeless dual boost (bridgeless boost) configuration is given in Figure 4. During the positive and negative cycles of the sinusoidal AC input voltage,  $Q_1$  and  $Q_2$  are switched on respectively. Boost inductor charges from the main supply through  $Q_1$  and body diode  $Q_2$  during the positive cycle. The stored energy of the inductor is discharged to the output capacitor through  $D_3$  and body diode  $Q_2$ . Inductor charges in the opposite direction for the negative cycle through  $Q_2$  and body diode of  $Q_1$ . Boost inductor discharges through  $D_4$  and body diode  $Q_1$  during the negative cycle. Only a single PWM gate pulse is enough to control the operation of both switches. High operating efficiency can be attained for low power applications and high power applications bridgeless interleaved boost converter is used.

Table 4 shows the designed values of the bridgeless boost converter with an output power of 500 W for an AC input voltage of 230 V, DC output voltage of 400 V, ripple voltage of 5% and ripple current of 10%. The detailed analysis of the different converter topologies reveal that a reconfigurable scheme can be implemented only in the case of a bridgeless boost converter. This is because the components used in this converter are so connected that they match the structure of VSI, which makes it easier for the switching operation.



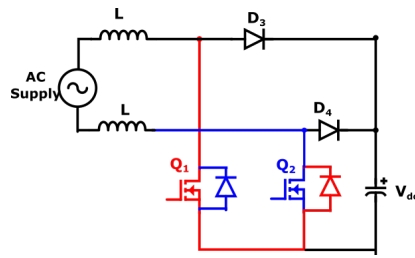


Figure 4. Bridgeless dual boost converter

Table 4. Design specification of bridgeless boost converter

Parameters	Symbols	Design equations	Design values
Dutycycle	$d$	$d = \frac{V_{dc} - V_{in}}{V_{dc}^{base}}$	0.425
Current	$I_{base}$	$I_{base} = \frac{P_c}{V_{base}}$	2.08 A
Switching frequency	$f_s$		20 kHz
Inductance	$L$	$L = \frac{V_{in} \times D}{\Delta I_L \times f_s}$	9 mH
Capacitance	$C_r$	$L = \frac{I_o \times D}{\Delta V_{out} \times f_s}$	1300 $\mu$ F

#### 4. PROPOSED RECONFIGURATION METHOD

A bridgeless boost PFC topology is realised by the reconfiguration of the propulsion motor drive as shown in Figure 5. Relay contactors (K1-K5) are used to disconnect VSI from the input battery and output propulsion motor for the charging operation. Since the contactors are operating for reconfiguration with zero current switching, fast switching devices are not required for this application instead of contactors. There are two operating modes for VSI based on the switching of relays. Propulsion mode: for the propulsion mode of operation, relays are in a normally closed (NC) position. K1 and K2 connect the VSI to the input battery side. K3, K4, and K5 connect the output of VSI to the traction motor side. The switching operation of VSI depends on the type of traction motor drive. The operation of switches VSI for a typical motor (BLDC motor) used in LEVs is given in Table 5.

Reconfiguration mode: the reconfiguration of VSI as an OBC is realised by energising the relay coil with an external pulse so that the coils move to the normally open (NO) position. Contactors at the normally open position, VSI is disconnected from the battery and the first two arms act as a bridgeless configuration and are connected to single phase AC supply using the relay contactors K3 and K4. Now VSI is reconfigured to act as front end bridgeless converter followed by a DC-DC converter for the battery charger. The switching operation is given in Table 6. The detailed mode of operation of VSI as a bridgeless PFC converter is given in Figure 6. The next section deals with the details of the experimental setup of the proposed method.

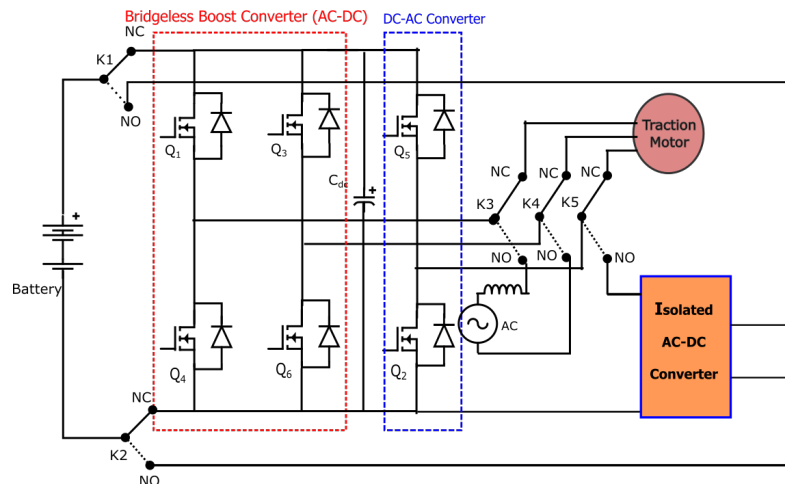


Figure 5. Reconfigurable VSI

Table 5. Switching states of VSI (propulsion mode)

Sector	Q1	Q2	Q3	Q4	Q5	Q6
I	0	1	1	0	0	0
II	0	0	1	1	0	0
III	0	0	0	1	1	0
IV	0	0	0	0	1	1
V	1	0	0	0	0	1
VI	1	1	0	0	0	0

Table 6. Switching states of first two legs of VSI (reconfiguration mode)

Input half cycle	Switch state (ON)	Switch state (OFF)
Positive Figure 6(a)	Q4,D6	Q1,Q3,Q6
Positive Figure 6(b)	D1, D6	Q1,Q3,Q6,Q4
Negative Figure 6(c)	Q6,D4	Q1,Q3,Q4
Negative Figure 6(d)	D3, D4	Q1,Q3,Q6,Q4

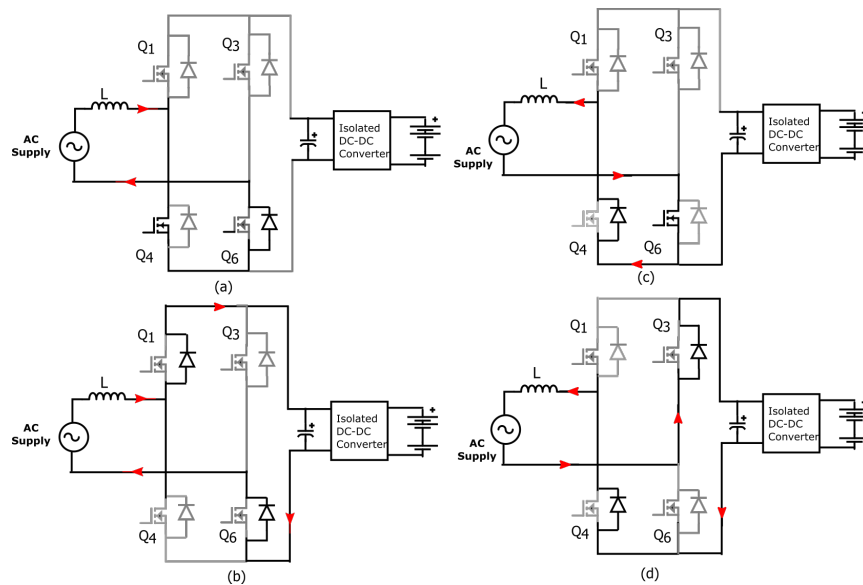


Figure 6. Modes of operation bridgeless dual boost converter: (a) positive half-cycle (Q4 and body diode of Q6 active), (b) positive half cycle (body diode of Q1 and body diode of Q6 conduction), (c) negative half-cycle (Q6 and body diode of Q4 active), and (d) negative half-cycle (body diode of Q3 and body diode of Q4)

## 5. EXPERIMENTAL VALIDATION

The experimental setup of a front end AC-DC rectifier using bridgeless dual boost topology is shown in Figures 7. A 750 W, 48 V BLDC motor is used as a traction motor for the experimental setup. Table 7 provides the specifications of the major components for the experimental setup. The voltage source inverter used as a traction motor drive is reconfigured to obtain a bridgeless dual boost converter. The first two legs of VSI act as AC -DC rectifier. PWM signal to control the switches is to be generated in synchronising with the input AC power supply.

Table 7. Major components for experimental setup

Item	Type/ specification
Li-ion battery	48 V, 24 Ah
Relay coil	Form 1C 30 A
Resonant controller	dsPIC33fJ32MC202
Power MOSFET	500 V, 30 A
Driver IC	IR2110
Triangular generator	IC 7038
Comparator	IC 741C
Optocoupler	PC817

The PWM generator circuit is shown in Figure 8. To generate PWM gating signals synchronised with the input AC power supply, Supply voltage is stepped down to 6 V and rectified using a precision rectifier. To control the modulation, the voltage gain of the rectified signal is varied by using an amplifier circuit. A triangular carrier signal is generated using function generator IC8038 and is compared with line synchronised

rectified sine wave to obtain the PWM signal using a comparator circuit. The line synchronised PWM signals are applied to the driver circuit with IR2110 and its output signal is used to drive the MOSFETs. VSI driver circuit using IR2110 can be used as the driver for the front end rectifier also. Hence additional driver circuit is not required. The reconfiguration and relay energisation steps are given in the flowchart shown in Figure 9.

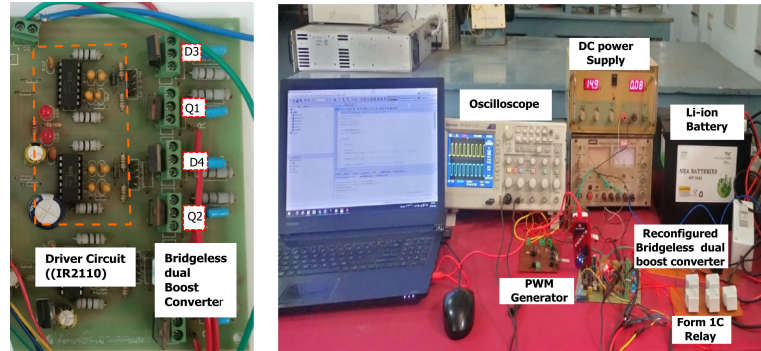


Figure 7. Hardware set up of bridgeless dual converter

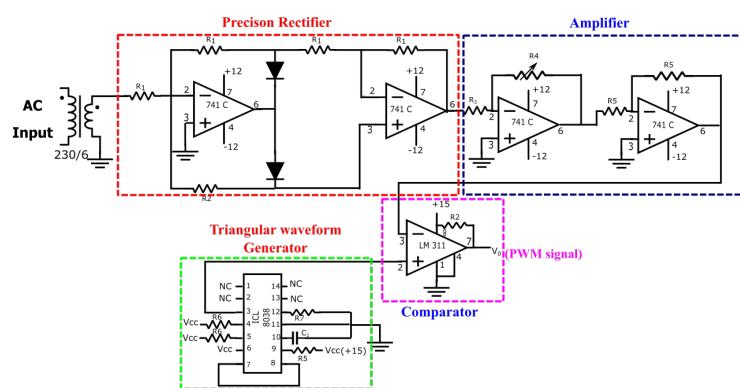


Figure 8. Control circuit to generate PWM signal for dual boost converter

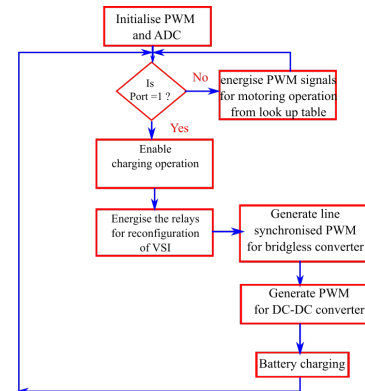


Figure 9. Relay energisation and steps for reconfiguration method

## 6. RESULTS AND DISCUSSION

In this paper, a detailed analysis of different bridgeless topologies is attempted as a first step and a comparison of these topologies with conventional diode bridge rectifiers with boost converters is done by simulation. The simulations are performed using the MATLAB-Simulink platform. As the next step, an experimental set up is made in which the selected converter topology is used. The following subsection deals with the results and its analysis.

### 6.1. Simulation results

The performance comparison of bridgeless topologies using simulation is presented in Figures 10(a)-10(d). It may be noted that the current distortion and thereby THD is high in the case of a conventional diode bridge rectifier with boost PFC converter, though reconfigurable. In the case of the bridgeless buck boost converter value of THD is low, but does not meet the requirements of IEC 61851 for charging EVs. Bridgeless Luo and bridgeless boost PFC converters provide comparable results with respect to their input current distortion characteristics and THD values.

It is clear from the comparison provided in Table 8 that the value of THD in the case of bridgeless Luo and bridgeless boost converters is low. Nevertheless, the bridgeless boost topology is chosen for further work, since it has the provision for the reconfiguration, which is the key requirement for the proposed scheme.

Moreover, a high value of 0.98 is obtained as the power factor as determined from the simulation result which is also an additional benefit of the selected topology.

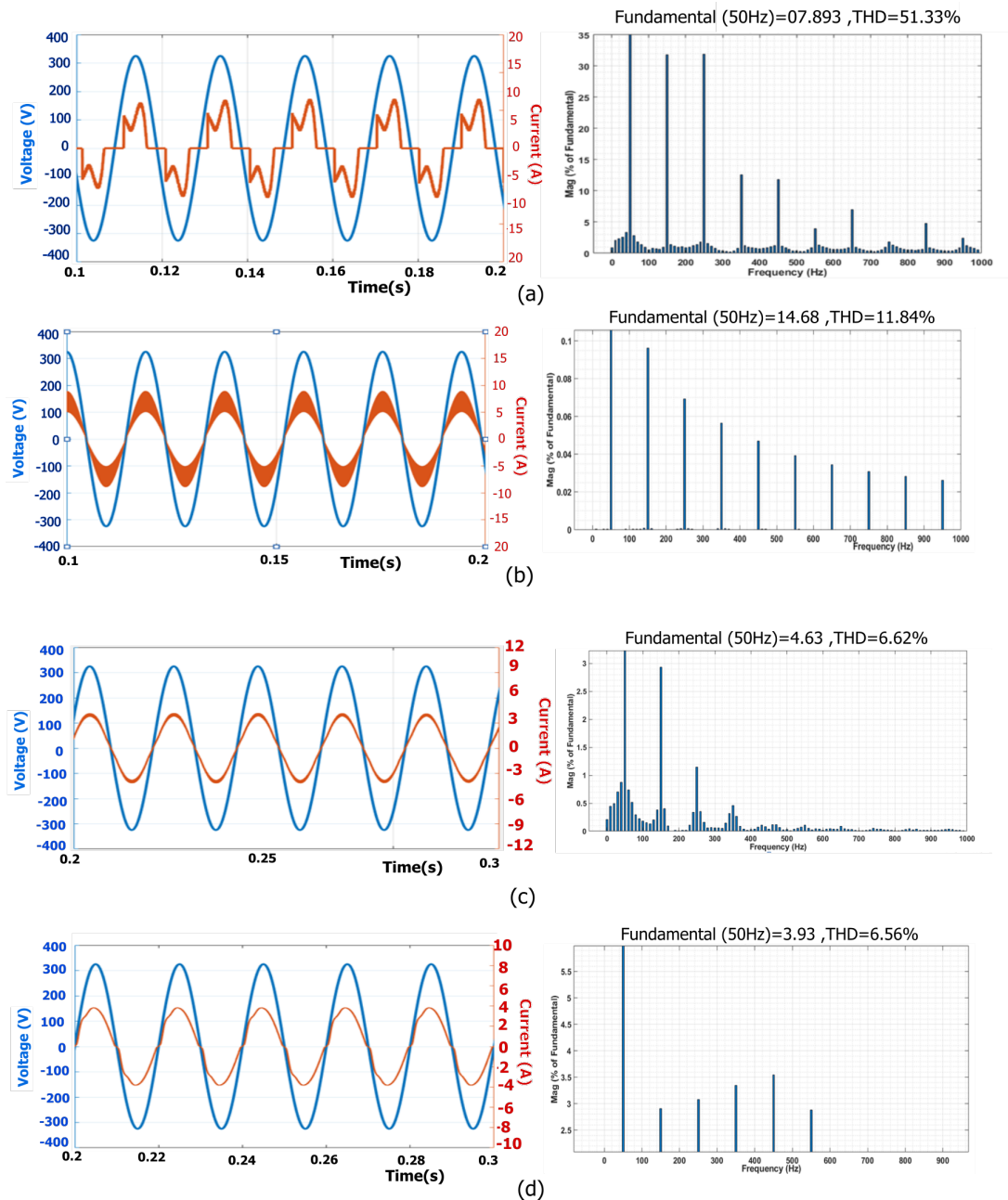


Figure 10. AC supply voltage and input current waveforms of PFC converter: (a) conventional diode bridge rectifier with boost converter, (b) bridgeless buck boost, (c) bridgeless Luo, and (d) bridgeless boost

Table 8. Comparison between different converters used for front end PFC

Topology	No. of switches	No. of diodes	No. of inductors	Bridgeless	Reconfigurable	THD (%)
Diode bridge rectifier + boost	1	5	1	No	Yes	51.33
Bridgeless buck boost	2	4	2	Yes	No	11.84
Bridgeless Luo	4	4	2	Yes	No	6.62
Bridgeless boost	2	2	2	Yes	Yes	6.56

## 6.2. Experimental results

The novel switching scheme proposed in section 4 is experimentally validated also. Figures 11(a)-11(b) shows the output of PWM signal generated from the comparator by comparing the sinusoidal signal with a triangular waveform. It produces PWM signals with constant switching frequency and variable pulse width depending on the variation in amplitude of the sinusoidal waveform. Figures 12(a)-12(b) shows the input current drawn by a conventional AC-DC rectifier using a diode bridge rectifier with a capacitor filter and the input current drawn by front end bridgeless boost PFC converter. The conventional circuit draws a peaky current and the waveform is non sinusoidal. But the bridgeless boost PFC converter draws an input current of sinusoidal in nature and reduces the distortion. This is an added advantage of using bridgeless boost converter.

Another merit of the selected converter topology is revealed by the factor named component utilisation factor (CUF), which is clear from Table 9. The utilisation factor of components measures the effectiveness of the reutilisation scheme and is used to compare the proposed integrated scheme with the existing schemes in literature. CUF of components is defined as the ratio of the minimum number of required components under the reconfiguration scheme to the actual number of components required. The higher value of CUF for both charging and propulsion modes with less number of switches for the proposed scheme is due to the reconfiguration of VSI, thereby reducing the number of components used. The reutilisation of VSI to integrate the battery charging operation also increases the power density and reduces the volume by reducing the number of switching devices. The major significance of the investigation provided in the paper is that based on the elaborate comparison of THD, CUF, and flexibility to reconfigure different converters, the best option is selected, so as to use it for different modes of operation of LEVs.

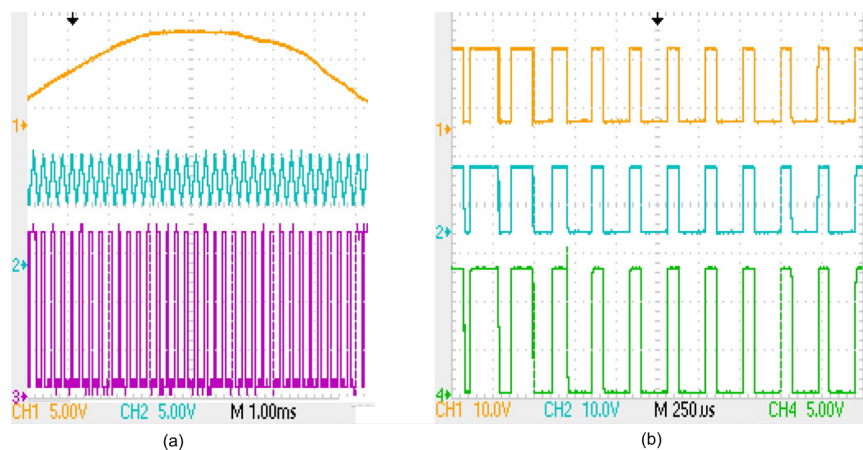


Figure 11. Control signals of front end AC-DC converter: (a) sinusoidal input, triangular carrier signal, and gate signals for lower MOSFETs from the comparator and (b) gate signals from the driver circuit, output of optocoupler

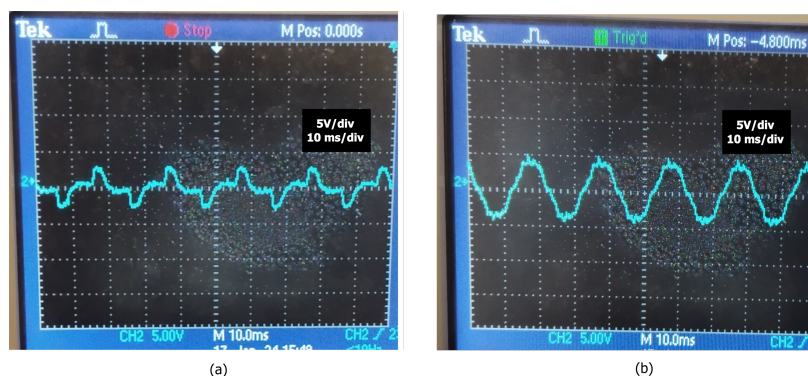


Figure 12. Input current drawn by the AC-DC converter: (a) waveform of input current drawn by conventional AC-DC rectifier and (b) waveform of input current drawn by bridgeless boost AC-DC rectifier

Table 9. Comparison of CUF of proposed integrated scheme with the other schemes available in recent research

Method	No.of switches (charging)	No.of switches (propulsion)	Total No.of switches	CUF (charging)	CUF (propulsion)
Scheme 1 [23]	16	12	16	1	0.75
Scheme 2 [30]	8	6	10	0.8	0.6
Scheme 3 [31]	21	6	21	1	0.29
Scheme 4 [32]	12	8	12	1	0.66
Proposed	8	6	8	1	0.75

## 7. CONCLUSION

An efficient and effective on-board battery charger is one of the main components in LEVs. The easiness of control, high power density, an improved front end power quality and input supply power factor enhance the performance of the overall system. Moreover, this leads to increased reliability and makes it more cost effective. A comprehensive study of different topologies of front end converters like conventional diode bridge rectifiers with boost, bridgeless buck boost, bridgeless Luo and bridgeless boost used for front end PFC in OBC is presented in this paper. A bridgeless boost PFC converter is selected owing to its obvious merits, as discussed based on the results obtained from the simulation. A novel switching scheme is also proposed, whereby the existing VSI is reconfigured into a PFC converter for battery charging mode so that the number of additional circuit elements is reduced. The front end power factor (0.98) and THD (6.56%) are improved to values as specified by IEC 61851 for charging EVs. The high value of the utilisation factor (0.75) with less number of switches also proves the significance of the proposed method. The experimental validation is also presented. As a future scope, a control for automatic switching from propulsion to charging modes can be developed, so as to make human intervention minimum in EVs. The feasibility of a bridgeless interleaved boost converter for high power applications with an additional reconfiguration circuit may also be investigated.

## REFERENCES




- [1] S. Krishnamoorthy and P. P. K. Panikkar, "A comprehensive review of different electric motors for electric vehicles application," *International Journal of Power Electronics and Drive Systems (IJPEDS)*, vol. 15, no. 1, pp. 74–90, 2024, doi:10.11591/ijpeds.v15.i1.pp74-90.
- [2] X. Sun, Z. Li, X. Wang, and C. Li, "Technology development of electric vehicles: A review," *Energies*, vol. 13, no. 1, p. 90, 2019, doi:10.3390/en13010090.
- [3] M. Ehsani, K. V. Singh, H. O. Bansal, and R. T. Mehrjardi, "State of the art and trends in electric and hybrid electric vehicles," *Proceedings of the IEEE*, vol. 109, no. 6, pp. 967–984, 2021, doi:10.1109/JPROC.2021.3072788.
- [4] A. K. Nayak, B. Ganguli, and P. M. Ajayan, "Advances in electric two-wheeler technologies," *Energy Reports*, vol. 9, pp. 3508–3530, 2023, doi:10.1016/j.egy.2023.02.008.
- [5] A. E. Aliasand and F. Josh, "Selection of motor for an electric vehicle: A review," *Materials Today: Proceedings*, vol. 24, pp. 1804–1815, 2020, doi:10.1016/j.matpr.2020.03.605.
- [6] B. Al-Hanahi, I. Ahmad, D. Habibi, and M. A. S. Masoum, "Charging infrastructure for commercial electric vehicles: Challenges and future works," *IEEE Access*, vol. 9, pp. 121476–121492, 2021, doi:10.1109/ACCESS.2021.3108817.
- [7] O. N. Nezamuddin, C. L. Nicholas, and E. C. d. Santos, "The problem of electric vehicle charging: State-of-the-art and an innovative solution," *IEEE Transactions on Intelligent Transportation Systems*, vol. 23, no. 5, pp. 4663–4673, 2022, doi:10.1109/TITS.2020.3048728.
- [8] A. Burkert and B. Schmuelling, "Comparison of two power factor correction topologies on conducted emissions in wireless power transfer systems for electric vehicles," in *2021 IEEE Vehicle Power and Propulsion Conference (VPPC)*, 2021, pp. 1–6, doi:10.1109/VPPC53923.2021.9699216.
- [9] S. S. Sayed and A. M. Massoud, "Review on state-of-the-art unidirectional non-isolated power factor correction converters for short-/long-distance electric vehicles," *IEEE Access*, vol. 10, pp. 11308–11340, 2022, doi: 10.1109/ACCESS.2022.3146410.
- [10] M. Bharathidasan and V. Indragandhi, "Review of power factor correction (pfc) AC/DC-DC power electronic converters for electric vehicle applications," in *IOP Conference Series: Materials Science and Engineering*, vol. 906, no. 1. IOP Publishing, 2020, p. 012006, doi: 10.1088/1757-899X/906/1/012006.
- [11] R. Patil and R. T. Ugale, "Comparative study of single-phase power factor correction topologies for electric vehicle battery charger based on boost converter," in *2022 IEEE Conference on Interdisciplinary Approaches in Technology and Management for Social Innovation (IATMSI)*, 2022, pp. 1–5, doi:10.1109/IATMSI56455.2022.10119337.
- [12] C. A. Sam and V. Jegathesan, "Bidirectional integrated on-board chargers for electric vehicles—a review," *S<sup>−</sup>adhan<sup>−</sup>a*, vol. 46, no. 1, p. 26, 2021, doi: 10.1007/s12046-020-01556-2.
- [13] E. Compatibility, "Limits for harmonic current emissions (equipment input current 16a per phase)," *IEC Standard IEC*, pp. 61 000–3, 2006.
- [14] R. Pandey and B. Singh, "A power factor corrected resonant ev charger using reduced sensor based bridgeless boost pfc converter," *IEEE Transactions on Industry Applications*, vol. 57, no. 6, pp. 6465–6474, 2021, doi: 10.1109/TIA.2021.3106616.






- [15] M. A. M. Noh, M. R. Sahid, T. K. Fei, and R. Lakshmanan, "Small-signal analysis of a single-stage bridgeless boost half-bridge AC/DC converter with bidirectional switch," *International Journal of Power Electronics and Drive Systems(IJPEDS)*, vol. 12, no. 4, pp. 2358–2371, 2021, doi:10.11591/ijpeds.v12.i4.pp2358-2371.
- [16] R. Meena Devi and L. Premalatha, "Analysis of bridgeless converter model for power factor correction," *Computers & Electrical Engineering*, vol. 87, p. 106785, 2020, doi:10.1016/j.compeleceng.2020.106785.
- [17] S. MaryAntony and G. Immanuel, "A novel single phase bridgeless AC/DC PFC converter for low total harmonics distortion and high power factor," *International Journal of Power Electronics and Drive Systems(IJPEDS)*, vol. 9, no. 1, pp. 17–24, 2018, doi:10.11591/ijpeds.v9.i1.pp17-24.
- [18] S. Hagbabin, S. Lundmark, M. Alakula, and O. Carlson, "Grid-connected integrated battery chargers in vehicle applications: Review and new solution," *IEEE Transactions on Industrial Electronics*, vol. 60, no. 2, pp. 459–473, 2012, doi: 10.1109/TIE.2012.2187414.
- [19] M. U. Deepa and G. R. Bindu, "A novel switching scheme for regenerative braking and battery charging for BLDC motor drive used in electric vehicle," in *2020 IEEE International Power and Renewable Energy Conference*, 2020, pp. 1–6, doi: 10.1109/IPRE-CON49514.2020.9315226.
- [20] T. Sutikno and S. Padmanabhan, "Integrated motor drive for vehicle electrification: a step toward a more sustainable and efficient transportation system," *International Journal of Power Electronics and Drive Systems(IJPEDS)*, vol. 14, no. 2, pp. 649–652, 2023, doi:10.11591/ijpeds.v14.i2.pp649-652.
- [21] T. Payarou and P. Pillay, "Integrated multipurpose power electronics interface for electric vehicles," *IEEE Transactions on Transportation Electrification*, vol. 9, no. 2, pp. 2429–2443, 2023, doi:10.1109/TTE.2022.3209098.
- [22] A. K. Gautam, M. Tariq, J. P. Pandey, K. S. Verma, and S. Urooj, "Hybrid sources powered electric vehicle configuration and integrated optimal power management strategy," *IEEE Access*, vol. 10, pp. 121 684–121 711, 2022, doi:10.1109/ACCESS.2022.3217771.
- [23] S. Semsar, T. Soong, and P. W. Lehn, "On-board single-phase integrated electric vehicle charger with v2g functionality," *IEEE Transactions on Power Electronics*, vol. 35, no. 11, pp. 12 072–12 084, 2020, doi:10.1109/TPEL.2020.2982326.
- [24] J. Johnson, T. Berg, B. Anderson, and B. Wright, "Review of electric vehicle charger cybersecurity vulnerabilities, potential impacts, and defenses," *Energies*, vol. 15, no. 11, p. 3931, 2022, doi:10.3390/en15113931.
- [25] S. Hemavathi and A. Shinisha, "A study on trends and developments in electric vehicle charging technologies," *Journal of energy storage*, vol. 52, p. 105013, 2022, doi:10.1016/j.est.2022.105013.
- [26] V. Bist and B. Singh, "An adjustable-speed PFC bridgeless buck–boost converter-fed BLDC motor drive," *IEEE Transactions on Industrial Electronics*, vol. 61, no. 6, pp. 2665–2677, 2013, doi: 10.1109/TIE.2013.2274424.
- [27] M. U. Deepa and G. R. Bindu, "Performance analysis of BLDC motor drive with power factor correction scheme," in *2016 IEEE International Conference on Power Electronics, Drives and Energy Systems (PEDES)*. IEEE, 2016, pp. 1–5, doi:10.1109/PEDES.2016.7914255.
- [28] B. Singh, V. Bist, A. Chandra, and K. Al-Haddad, "Power factor correction in bridgeless-Luo converter-fed BLDC motor drive," *IEEE Transactions on Industry Applications*, vol. 51, no. 2, pp. 1179–1188, 2014, doi: 10.1109/TIA.2014.2344502.
- [29] J. Gupta and B. Singh, "Bridgeless isolated positive output Luo converter based high power factor single stage charging solution for light electric vehicles," *IEEE Transactions on Industry Applications*, vol. 58, no. 1, pp. 732–741, 2021, doi: 10.1109/TIA.2021.3131647.
- [30] C. Shi, Y. Tang, and A. Khaligh, "A single-phase integrated onboard battery charger using propulsion system for plug-in electric vehicles," *IEEE Transactions on Vehicular Technology*, vol. 66, no. 12, pp. 10 899–10 910, 2017, doi: 10.1109/TVT.2017.2729345.
- [31] C. Shi and A. Khaligh, "A two-stage three-phase integrated charger for electric vehicles with dual cascaded control strategy," *IEEE Journal of Emerging and Selected Topics in Power Electronics*, vol. 6, no. 2, pp. 898–909, 2018, doi: 10.1109/TPEL.2017.2727398.
- [32] O. Hegazy, J. Van Mierlo, and P. Lataire, "Control and analysis of an integrated bidirectional DC/AC and DC/DC converters for plug-in hybrid electric vehicle applications," *Journal of Power Electronics*, vol. 11, no. 4, pp. 408–417, 2011, doi: 10.6113/JPE.2011.11.4.408.

## BIOGRAPHIES OF AUTHORS



**Deepa Machadan Unni**    is an assistant professor in the Department of Electrical Engineering, College of Engineering Trivandrum, Kerala, India. She received her B.Tech. degree in Electrical and Electronics Engineering from Calicut University, Kerala in 2005, her M.Tech. degree in Industrial Drives and Control from M G University, Kerala in 2010 and currently doing Ph.D. at University of Kerala, India. Her research interests include power electronics, motor drives, and electric vehicles. She can be contacted at email: deepashibu@cet.ac.in.



**Bindu Gopakumar Rajalekshmi**    is a former principal of Government Engineering College Thrissur, Kerala, India. She also served as head of the Department of the Department of Electrical Engineering and the dean of the College of Engineering Trivandrum, Kerala, India. She has a teaching experience of 30 years in various engineering colleges in Kerala, India. She has more than 125 research publications to her credit, with more than 1000 citations as per Google Scholar metrics. Her research areas include control of electrical machines, electromagnetics, and soft computing. She can be contacted at email: bgr@cet.ac.in.